

Identification of a Nonbasic, Nitrile-Containing Cathepsin K Inhibitor (MK-1256) that is Efficacious in a Monkey Model of Osteoporosis

Jöel Robichaud,[†] W. Cameron Black,[†] Michel Thérien,[†] Julie Paquet,[†] Renata M. Oballa,[†] Christopher I. Bayly,[†] Daniel J. McKay,[†] Qingping Wang,[†] Elise Isabel,[†] Serge Léger,[†] Christophe Mellon,[†] Donald B. Kimmel,[‡] Gregg Wesolowski,[‡] M. David Percival,[†] Frédéric Massé,[†] Sylvie Desmarais,[†] Jean-Pierre Falgoutyret,[†] and Sheldon N. Crane^{*†}

Merck Frosst Centre for Therapeutic Research, 16711 Trans Canada Highway, Kirkland, Quebec, Canada, H9H 3L1, and Merck Research Laboratories, West Point, Pennsylvania 19486

Received May 22, 2008

Herein, we report on the identification of nonbasic, potent, and highly selective, nitrile-containing cathepsin K (Cat K) inhibitors that are built on our previously identified cyclohexanecarboxamide core structure. Subsequent to our initial investigations, we have found that incorporation of five-membered heterocycles as P2–P3 linkers allowed for the introduction of a methyl sulfone P3-substituent that was not tolerated in inhibitors containing a six-membered aromatic P2–P3 linker. The combination of a five-membered *N*-methylpyrazole linker and a methyl sulfone in P3 yielded subnanomolar Cat K inhibitors that were minimally shifted (<10-fold) in our functional bone resorption assay. Issues that arose because of metabolic demethylation of the *N*-methylpyrazole were addressed through introduction of a 2,2,2-trifluoroethyl substituent. This culminated in the identification of **31** (MK-1256), a potent (Cat K IC₅₀ = 0.62 nM) and selective (>1100-fold selectivity vs Cat B, L, S, C, H, Z, and V, 110-fold vs Cat F) inhibitor of cathepsin K that is efficacious in a monkey model of osteoporosis.

Introduction

As the majority of individuals comprising the baby-boomer generation reach retirement age and enter their golden years, Western society will become increasingly burdened with the demands of addressing the medical needs of its sizable elderly population. Many of these challenges will arise as a result of the metabolic changes inherent in the process of aging, such as those experienced by postmenopausal women following the loss of ovarian sex steroid production. One of the consequences of this particular physiological alteration is increased rates of bone resorption relative to bone formation. Left untreated, the resulting loss in bone mass places the individual in a state of skeletal fragility and increased susceptibility to hip, spine, and wrist fractures. This condition, commonly known as osteoporosis, currently afflicts about 8 million women in the U.S. and is one of the leading causes of morbidity and mortality in women over 50 years of age. A fact that is less appreciated by the population at large is that this condition also affects approximately 2 million men in the U.S. Although males are less vulnerable to osteoporosis because of their greater peak bone mass and the fact that they do not experience an abrupt loss of gonadal sex steroids, the mortality rate associated with hip fracture for men is twice that for women. Thus, osteoporosis represents a significant health challenge for elderly individuals of both sexes.^{1a,b}

Regardless of the underlying causative factors, osteoporosis ultimately arises in both males and females as a result of an increased activity of the bone resorbing cell, the osteoclast, relative to its bone forming counterpart, the osteoblast.^{2a,b} Currently available treatment regimens for osteoporosis can be separated into two classes depending on which cell type they exert their effect. The bone forming agents such as injectable

recombinant parathyroid hormone (PTH^c) and strontium ranelate target the osteoblast, while the antiresorptive therapies that target the osteoclast include hormone-replacement therapy (HRT), selective estrogen receptor modulators (SERMS), calcitonin, and the bisphosphonates.^{3a,b} The most widely prescribed therapy for osteoporosis, the bisphosphonate class of antiresorptives, halts osteoclast activity and allows for the existing resorption spaces generated by the osteoclast to be filled in with new bone by the unaffected osteoblast. Placebo-controlled studies with bisphosphonates in postmenopausal women have repeatedly demonstrated fracture reduction efficacy of ~40–50% for both vertebral and nonvertebral fractures.^{1a,b} The bisphosphonates are currently the preferred therapy for osteoporosis by virtue of their long-term safety (>10 years) and superior efficacy relative to the other available treatments in fracture reduction trials.^{3a,b} The ideal therapeutic strategy would serve to rebuild lost bone while re-establishing the physiological balance between osteoclast and osteoblast activity. Thus, we have been actively seeking to develop antiresorptive agents that, unlike bisphosphonates, uncouple these two processes to favor bone formation over resorption.

A little over a decade ago, biochemical and genetic evidence began to surface that implicated the cysteine protease cathepsin K (Cat K) as a key player in the process of bone resorption by osteoclasts.⁴ This stimulated a vigorous research effort within the pharmaceutical industry aimed at the development of Cat K inhibitors for the treatment of osteoporosis and other disorders

* To whom correspondence should be addressed. Phone: 514-428-3934. Fax: 514-428-2624. E-mail: sheldon_crane@merck.com.

[†] Merck Frosst Centre for Therapeutic Research.

[‡] Merck Research Laboratories.

^a Abbreviations: Cat, cathepsin; hrb, humanized rabbit; rab, rabbit; P1, P2, P3, peptide subsites 1, 2, and 3; S1, S2, S3, protease subsites 1, 2, and 3; PTH, parathyroid hormone; HRT, hormone replacement therapy; SERMS, selective estrogen receptor modulators; BRS, bone resorption shift; PK, pharmacokinetic; CYP, cytochrome P450; HATU, 2-(1*H*-7-azabenzotriazol-1-yl)-1,1,3,3-tetramethyluronium hexafluorophosphate; OVX, ovariectomized; ELISA, enzyme-linked immunosorbent assay; NTx, N-terminal telopeptide collagen degradation fragment; u-NTx, urinary N-terminal telopeptide collagen degradation fragment; CTx, C-terminal telopeptide collagen degradation fragment; Cre, creatinine; qd, once daily; po, oral; NS, not significant; SW, saline wash.

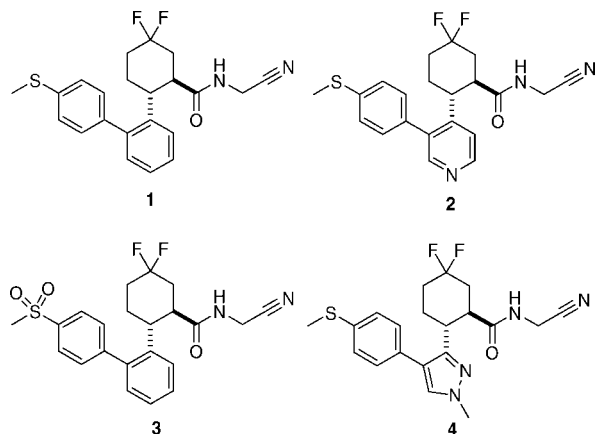


Figure 1. *gem*-Difluorocyclohexylcarboxamide cathepsin K inhibitors of varying polarity.

characterized by pathophysiological bone loss. Indeed, efforts from our own laboratories have led to the identification of odanacatib, a potent and selective Cat K inhibitor, that is currently in phase III clinical trials for osteoporosis.^{5a} We have recently disclosed the results of our preliminary investigations aimed at developing a Cat K inhibitor built upon the cyclohexanecarboxamide scaffold.^{6a,b} Herein, we report on the successful identification of an orally available, small molecule inhibitor from this distinct structural class.

Background and Key Issues

The major impasse hindering identification of a development candidate from the cyclohexanecarboxamide series was a substantial loss of potency (50- to 100-fold) in our bone resorption assay utilizing rabbit osteoclasts^{7a} relative to activity against isolated rabbit Cat K. During the early stages of our research program, we had observed that cathepsin K inhibitors of comparable intrinsic potency could exhibit disparate levels of efficacy in our *in vivo* animal models at equivalent plasma exposure levels. Invariably, it was ascertained that higher levels of *in vivo* efficacy were observed for those Cat K inhibitors that were more potent in our bone resorption assay. Thus, minimization of this potency loss, formally defined here as the bone resorption shift (BRS = (rabbit bone resorption IC₅₀)/(rabbit Cat K IC₅₀)), represented a key facet of our research effort. The BRS value was also utilized to calculate the projected monkey and human bone resorption IC₅₀ values in lieu of monkey and human versions of the bone resorption assay.^{7b} For the cyclohexylcarboxamide series of compounds, it appeared unlikely that nonspecific binding to serum proteins present in the assay media was solely responsible for an increase in BRS, as representative compound **1** (Figure 1) was found to be shifted 53-fold in the functional assay despite being only moderately bound (85%) to rat, rabbit, and human plasma proteins as determined by ultracentrifugation.⁸ In general, it was observed that as the polarity of our Cat K inhibitors increased, the BRS value decreased. Recently, we reported that replacement of the P2–P3⁹ phenyl linker in **1** with more polar functionality such as a pyridine in **2** served to ameliorate the undesirable potency shift, regrettably at the expense of Cat K potency, counterscreen selectivity, and pharmacokinetic (PK) properties.^{6b} Subsequent to this, we discovered that a variety of Cat K inhibitors incorporating a methyl sulfone (**3**) instead of a methyl thioether (**1**) in P3 were shifted only 8- to 10-fold in our functional assay. Unfortunately, these gains were offset by an 85-fold reduction in potency in this instance (humanized rabbit Cat K^{10a,b} IC₅₀ of 0.28 and 24 nM, respectively).

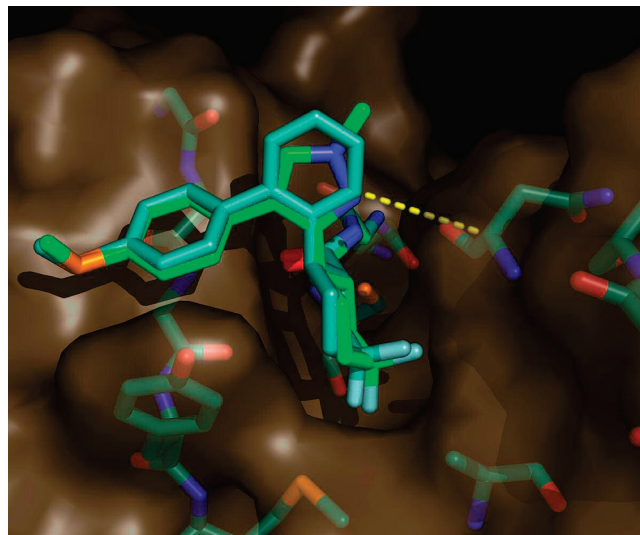


Figure 2. Modeled structures of inhibitors **1** (gray) and **4** (green) bound to the active site of cathepsin K.

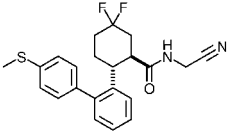
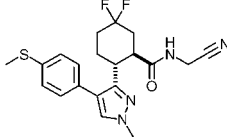
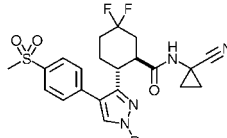
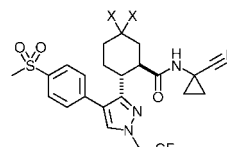
Explicit solvent molecular dynamics calculations, conducted using the AMBER suite of programs,¹¹ suggested that switching from a six- to a five-membered heteroaromatic P2–P3 linker such as an *N*-methylpyrazole in **4** could allow for improved binding to humanized rabbit Cat K^{10a} by virtue of reduced steric contact of the inhibitor with Asn158 in S2 (dashed line in Figure 2). More importantly, this structural modification was expected to lift the sulfur atom of the P3-methyl thioether substituent away from the enzyme surface in S3. Thus, it was reasoned that the more sterically demanding methyl sulfone functionality would be better accommodated in P3 upon switching to a five-membered heteroaromatic linker.

In order to test this idea, a methyl sulfone was incorporated into P3 of **4**. This structural modification resulted in a mere 2- to 4-fold decrease in humanized rabbit Cat K potency in contrast with the 85-fold loss observed for **3**, thereby validating the molecular modeling hypothesis. Compound **5**, incorporating the pyrazole linker and methyl sulfone in P3, represented the first subnanomolar Cat K inhibitor from the cyclohexanecarboxamide class that was shifted less than 10-fold in the bone resorption assay (Table 1).

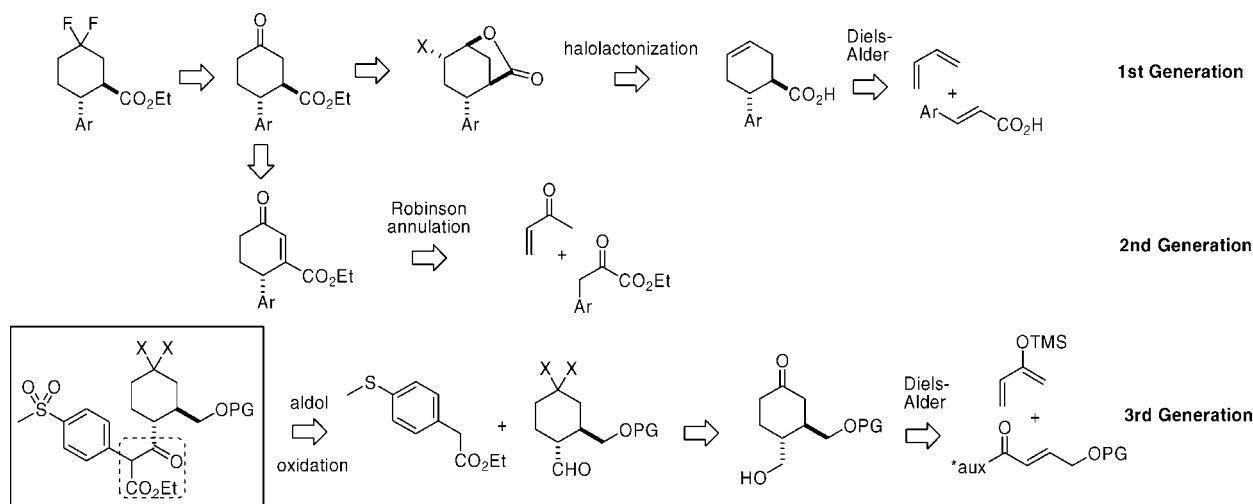
Compound **5** exhibited a half-life in rats comparable to its progenitor **4** (*T*_{1/2} of 4.6 and 4.1 h, respectively). Exchange of the P3-methyl thioether in **4** for a methyl sulfone in **5** and introduction of a cyclopropyl in P1 circumvented oxidative metabolism in those regions of the inhibitor. However, the methyl of the *N*-methylpyrazole in **5** was found to be susceptible to CYP-mediated oxidation. This generated the active metabolite **6** that was observed to be circulating during *in vivo* studies. Owing to the success of the fluorination of the cyclohexyl ring as a strategy to reduce oxidative metabolism,^{6a} it seemed logical to employ a similar tactic to address the issues associated with the oxidative demethylation of pyrazole **5**. It was anticipated, based in Figure 2, that a wide variety of substituents would be tolerated on the pyrazole nitrogen owing to orientation of this region of the enzyme-bound inhibitor toward bulk solvent.

Compounds incorporating a pyrazole P2–P3 linker such as **5** could be prepared using either the Diels–Alder (first generation)^{6a} or Robinson annulation (second generation)^{6b} based strategies reported previously by us (Figure 3). However, these synthetic approaches were limiting in that an intact aromatic group was required in the key building block and thereby lacked the end-game flexibility required to study a

Table 1. Potency and Selectivity Profiles of Selected Cathepsin K Inhibitors

Structure	hrab Cat K ^{10a} IC ₅₀ (nM) ^a	rabCat K IC ₅₀ (nM) ^a	Selectivity Ratios ^{a,b}			Bone Res IC ₅₀ (nM) ^a	BRS ^c (fold)
			Cat L/K	Cat B/K	Cat S/K		
 (<i>R,R</i>)-1	0.28	0.32	780	>36000	940	16	53
 rac-4	0.37	0.41	730	9500	490	41	100
 (<i>R,R</i>)-5 R = CH ₃	0.81	4.5	4500	4400	1200	35	8
(<i>R,R</i>)-6 R = H	1.8	18.6	4900	2900	2300	120	7
 (<i>R,R</i>)-30 X = F	0.69	9.3	9500	>14000	7100	51	6
(<i>R,R</i>)-31 X = Cl	0.62	6.1	4700	>16000	4300	50	8

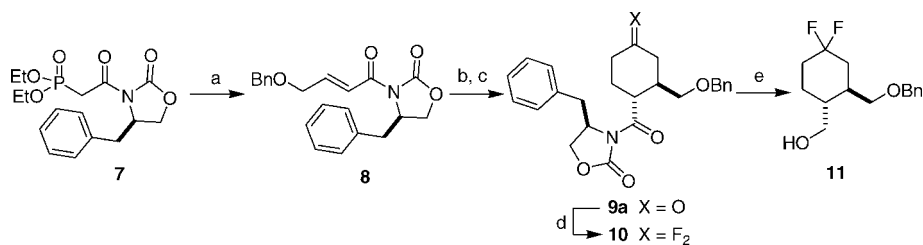
^a Each value represents an average of at least three independent determinations. ^b Counterscreen assays were performed using human Cat L, B, and S. ^c Bone resorption shift BRS = (bone resorption IC₅₀)/(rabCatK IC₅₀).

**Figure 3.** Strategies for the synthesis of cyclohexylcarboxamide cathepsin K inhibitors.

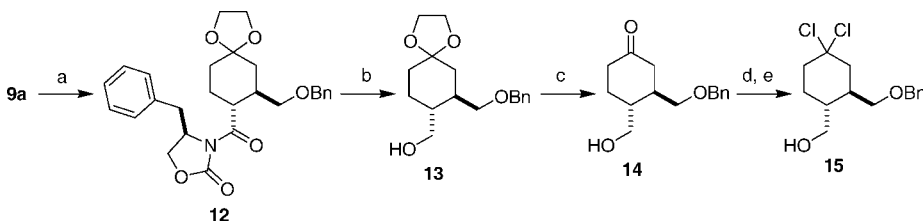
variety of heteroaromatic P2–P3 linkers. In addition, our previous generation syntheses often relied on cumbersome HPLC-based resolution procedures to produce the desired Cat K inhibitors in high enantiopurity. In order to effectively deal with the issues related to the oxidative demethylation of **5**, a more flexible, third generation enantioselective synthetic route was required.

Chemistry

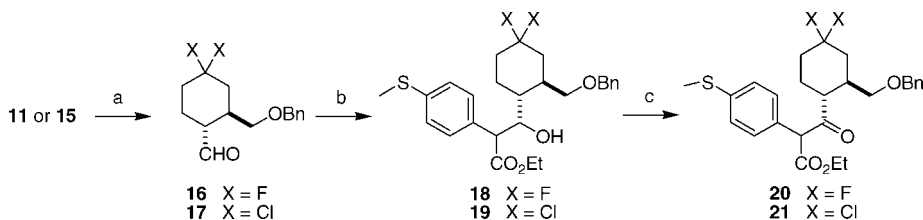
A strategy was devised that would allow for access to a wide variety of heterocyclic P2–P3 linkers, with a focus on N-substituted pyrazoles, from a late-stage keto-ester intermediate (boxed in Figure 3). At the same time, we were mindful to incorporate the *gem*-difluoro substituent that proved crucial for controlling oxidative metabolism on the P2-cyclohexane portion

Scheme 1^a

^a Conditions: (a) BnOCH_2CHO , $i\text{-Pr}_2\text{NEt}$, LiCl , CH_3CN ; (b) 2-[(trimethylsilyloxy)-1,3-butadiene, Et_2AlCl , CH_2Cl_2 , -78°C ; (c) 6 M HCl , -40°C to room temp, 45% over three steps; (d) $(\text{MeOCH}_2\text{CH}_2)_2\text{NSF}_3$, CH_2Cl_2 , 0°C , 43%; (e) BuLi , benzyl mercaptan, 0°C , then LiAlH_4 , 96%.

Scheme 2^a

^a Conditions: (a) 1,2-bis[trimethylsilyloxy]ethane, TMSOTf , CH_2Cl_2 , room temp, >99%; (b) BuLi , ethanethiol, 0°C , then LiAlH_4 , 86%; (c) AcOH , H_2O , 85°C , 95%; (d) $\text{H}_2\text{NNH}_2 \cdot \text{H}_2\text{O}$, MeOH , 4 Å sieves; (e) CuCl_2 , Et_3N , MeOH , 0°C , 76%.

Scheme 3^a

^a Conditions: (a) DMP , CH_2Cl_2 , 86% for **16**, 78% for **17**; (b) ethyl 4-(methylthio)phenylacetate, LDA , THF , -78°C , 56% for **16**, 80% for **17**; (c) oxalyl chloride, DMSO , Et_3N , CH_2Cl_2 , -78°C to room temp, 88% for **20**, 97% for **21**.

of these inhibitors. We also prepared the corresponding *gem*-dichloro analogue, as molecular modeling studies suggested that a *gem*-dichlorocyclohexyl in conjunction with a five-membered heterocyclic linker should be tolerated in the active site of Cat K.

Our third generation synthesis begins in Scheme 1 with preparation of dienophile **8**¹² for utilization in an Evan's auxiliary-controlled Diels–Alder reaction¹³ with 2-[(trimethylsilyloxy)-1,3-butadiene. This sequence yielded the desired cyclohexanone **9a** following in situ hydrolysis of the initially formed enol-silyl ether. Some of the corresponding diastereomeric cyclohexanone **9b**, epimeric at the both the imide and benzyl ether bearing stereocenters, was also formed from this reaction sequence (ratio of **9a/9b** = 7:1). However, the major diastereomer **9a** proved to be more crystalline than the minor isomer and could be separated by precipitation from a mixture of ethyl acetate and hexanes on a larger scale. On a smaller scale, quantitative separation was readily achieved by conventional flash chromatography. Introduction of the *gem*-difluoro substituent in **10** was accomplished by treatment of **9a** with Deoxofluor. Subsequent cleavage of the Evan's auxiliary with lithium benzylmercaptide and reduction of the intermediate thioester with LiAlH_4 generated alcohol **11**.¹⁴

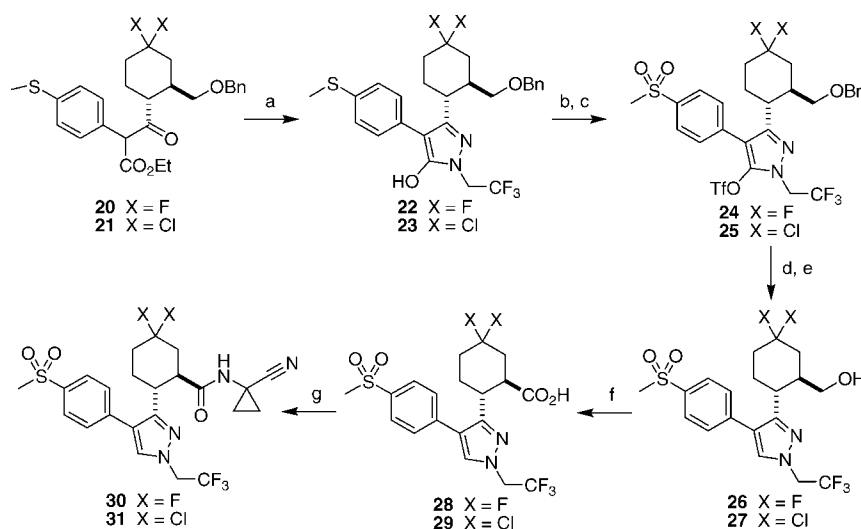
Preparation of the corresponding *gem*-dichloro alcohol required an alternative sequence of events (Scheme 2), as the acyloxazolidinone functionality did not tolerate the conditions used below for conversion of a ketone into a *gem*-dichloro group. Thus, the acyloxazolidinone in **9a** was first converted into the corresponding primary alcohol **13** according to the

method described above, after first protecting the ketone functionality as a 1,3-dioxolane in **12**. Cleavage of the ketal protecting group with wet acetic acid at 85°C liberated the ketone in **14** that was subsequently transformed to a *gem*-dichloro in **15** via treatment of the intermediate hydrazone with CuCl_2 and Et_3N .¹⁵

Alcohols **11** and **15** were transformed into the corresponding aldehydes **16** and **17** by oxidation with Dess–Martin periodinane (Scheme 3). Reaction of the aldehydes with the carbanion generated from ethyl 4-(methylthio)phenylacetate and LDA yielded alcohols **18** and **19**, which were converted via a Swern oxidation to the key keto-ester intermediates **20** and **21** targeted in Figure 3.

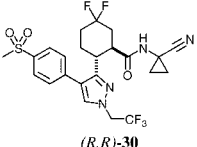
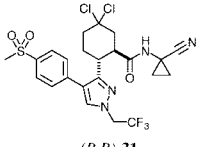
With keto-esters **20** and **21** in hand, we were in a position to prepare a variety of heterocyclic analogues of **5** using classical heterocyclic chemistry methodology.¹⁶ As mentioned above, the corresponding *N*-trifluoroethylpyrazole analogues were initially targeted for synthesis from keto-esters **20** and **21** (Scheme 4).

Heating of **20** and **21** with trifluoroethylhydrazine and MgSO_4 in refluxing toluene produced hydroxypyrazoles **22** and **23**. The hydroxyl oxygen was subsequently activated for removal by conversion to the corresponding triflate, and the methyl thioether was oxidized to a methyl sulfone in **24** and **25** with *m*-CPBA. Exposure **24** and **25** to an atmosphere of hydrogen gas in the presence of 10% Pd/C in methanol containing triethylamine effected the necessary deoxygenation to complete the construction of the *N*-trifluoroethylpyrazole P2–P3 linker. Removal of the benzyl ether protecting group was smoothly effected with hydrogen in the presence of Pearlman's catalyst and acetic acid

Scheme 4^a

^a Conditions: (a) $\text{CF}_3\text{CH}_2\text{NHNH}_2$, PhMe, MgSO_4 , reflux, 81% for **22**, 64% for **23**; (b) TiF_2O , pyr, CH_2Cl_2 ; (c) *m*CPBA, CH_2Cl_2 , 0°C to room temp, 96% for **24**, 90% for **25**; (d) H_2 , 10% Pd/C, Et_3N , EtOAc, 3 Å molecular sieves; (e) H_2 , 10% Pd(OH)₂/C, EtOAc, AcOH, 66% for **26**, 60% for **27** over two steps; (f) Jones' reagent, acetone, 0°C; (g) 1-aminocyclopropylacetonitrile hydrochloride, HATU, Hünig's base, DMF, room temp, 82% for **30**, 91% for **31** over two steps.

Table 2. Pharmacokinetic Profiles of *N*-Trifluoroalkylpyrazole-Containing Cathepsin K Inhibitors

Compound	Species	%F	Cl (mL/min/kg)	T _{1/2} (h)	V _d (L/kg)
 (R,R)-30	Rat	25	14	4.4	3.2
	Dog	31	1.8	7.8	1.2
 (R,R)-31	Rat	105	7.8	4.4	2.8
	Dog	60	1.4	34	2.1
	Rh. Monkey	104	5	13	3.4

in ethyl acetate. Attempts to accomplish these two transformations in a single operation using either of the palladium catalysts were not successful. Jones' oxidation of the liberated primary alcohols **26** and **27** and HATU-mediated coupling of the carboxylic acid products **28** and **29** to 1-aminocyclopropylacetonitrile concluded the synthetic sequence and provided the enantiopure *N*-trifluoroethylpyrazole analogues **30** and **31** for evaluation in our barrage of in vitro and in vivo assays.

Potency and Counterscreen Selectivity

As shown in Table 1, compounds **30** and **31** were ascertained to be subnanomolar inhibitors of humanized rabbit Cat K and, like other inhibitors possessing a methyl sulfone in P3,^{5a,b} were less than 10-fold shifted in the functional bone resorption assay (BRS = 6 and 8, respectively). No appreciable loss of potency or selectivity was observed by switching from a *gem*-difluoro in **30** to a *gem*-dichloro in **31**, in contrast to the situation described previously with **1**.^{6a} Relative to *N*-methylpyrazole **5**, the *N*-(2,2,2-trifluoroethyl) analogues exhibited similar potencies against humanized rabbit Cat K and comparable selectivities against human cathepsins B, L, and S. Compounds **30** and **31** were also quite selective against a wider panel of human

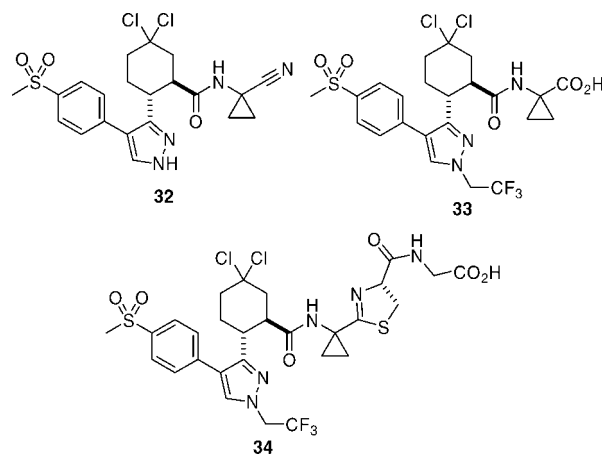


Figure 4. Metabolites generated from **31** in rats.

lysosomal cysteine proteases including human cathepsins C (6000-fold), H (>14000-fold), Z (1700-fold), and V (1100-fold). Compounds **30** and **31** were also selective against human cathepsin F but to a lesser degree (110-fold).

Pharmacokinetics and Metabolism

Both **30** and **31** displayed acceptable PK profiles in multiple animal species (Table 2). *gem*-Dichloro analogue **31** was ultimately selected for metabolism and excretion profiling on the basis of its superior bioavailability and half-life.

Rat plasma samples from PK studies and the assay medium from compound incubations conducted with freshly isolated rat hepatocytes were analyzed by LC-MS. From these experiments, it was ascertained that **31** was subject to less than 1% oxidative metabolism. Similar observations were also made during human hepatocyte incubations. In order to fully characterize the metabolic fate of **31** in rats, excretion studies were conducted with radiolabeled compound¹⁷ introduced orally in bile-cannulated animals. During these experiments, it was demonstrated that after 96 h, the total amount of recovered radioactivity was quite high, with 92% of the dosed radioactivity being recovered from the bile (16%), urine (18%), and feces (58%). In bile samples collected between 2 and 4 h postdosing, the parent drug

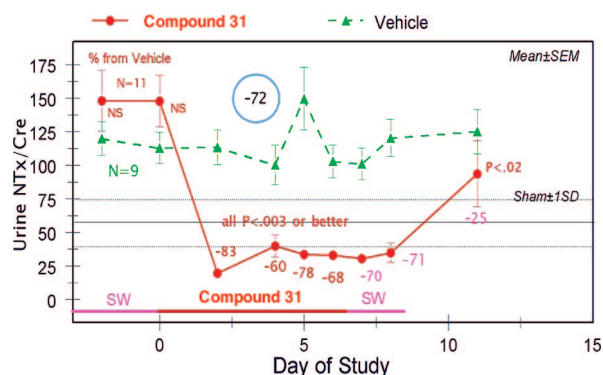


Figure 5. Urinary NTx/Cre during 1 mpk compound **31** po, q.d. adult OVX rhesus monkeys. Compound **31** reduces bone resorption in OVX rhesus monkeys. Bone resorption in OVX monkeys treated with compound **31** (●) or vehicle (▲) was evaluated using the urine biochemical marker NTx. Data are reported as uNTx/creatinine (nM/mM).

and three main metabolites were detected by radio-HPLC analysis. These metabolites were identified by LC-MS as the dealkylated pyrazole **32**, the nitrile hydrolysis product **33**, and the Cys-Gly conjugate **34** (Figure 4). The latter two metabolites were likely generated through the mercapturic acid biotransformation pathway.^{18a,b} Of the total recovered radioactivity, 90% was attributed to unchanged parent **31** with the metabolites constituting the remaining 10%. The dealkylated pyrazole **32** was found to comprise only 0.1% of the total recovered radioactivity. Thus, oxidative metabolism did not significantly contribute to the clearance of **31** during rat PK studies, consistent with the observations made during hepatocyte incubations. This was not surprising given the fact that the three sites susceptible to oxidative metabolism in earlier generation inhibitors, namely, the cyclohexyl ring, the substituent on nitrogen of the pyrazole, and the methylene adjacent to the nitrile warhead, have all been suitably modified to circumvent this in **31**.

Pharmacology

Ovariectomized (OVX) monkeys experience estrogen deficiency and accelerated bone loss analogous to postmenopausal women.^{19a} Assessment of the magnitude of bone turnover can be achieved through ELISA-monitoring of the bone resorption biomarkers CTx and NTx in serum and/or urine. Thus, evaluation of the effect of compound treatment on bone resorption biomarkers relative to untreated control animals constitutes a rapid measure of biochemical efficacy of the pharmacological agent of interest in an osteoporotic context.^{19b} On the basis of data obtained during a study of the pharmacokinetic behavior of **31** in rhesus monkeys (Table 2), it was predicted that a dose of 1 mpk would provide trough levels ($t = 24$ h) near the projected monkey bone resorption IC_{50} value of 2 nM.^{7b} Under the above experimental paradigm, once-daily (qd) oral administration of **31** at 1 mpk for a period of 1 week achieved a mean 72% reduction (Figure 5) of urinary-*N*-telopeptide fragment levels (u-NTx, normalized to creatine output). The mean plasma concentrations of **31** measured on the final day of dosing for this study were as follows: $C_{max} = 400$ nM ($T_{max} = 4$ h), $C_{24h} = 80$ nM, $AUC = 4.2 \mu M \cdot h$. This magnitude of bone turnover marker suppression is comparable to that seen for other nitrile-based inhibitors of Cat K, such as our first generation dipeptide inhibitor L-006,235 (76% u-NTx reduction at 15 mpk/qd)^{5c} and our nonbasic trifluoroethylamine based inhibitor L-873,724

(68% u-NTx reduction at 3 mpk/qd),^{5b} which is structurally similar to our clinical candidate odanacatib.^{5a}

Kinetic Characterization

The reversibility of inhibition of humanized rabbit Cat K by **31** was demonstrated in experiments in which a 1:1 enzyme-inhibitor mixture (0.12 μM) was preincubated for 15 min, followed by a 500-fold dilution into substrate-containing buffer (0.2 μM citrate). After dilution, the Cat K enzyme activity was initially >99% inhibited and slowly recovered with a $t_{1/2} = 215$ s to a velocity similar to that of the control incubation, demonstrating the reversibility of the formation of the **31**-cathepsin K complex.

Discussion

It is widely accepted that bisphosphonate antiresorptives exert their effects on osteoclasts via disruption of the mevalonic acid pathway following selective uptake of the bone-immobilized bisphosphonate.^{3b} The ensuing dysfunction and ultimate apoptotic demise of the osteoclast then effect the management of excessive bone resorption. The intricate process that constitutes the maintenance of normal bone structure relies on the coordinated action of both the osteoclast and the osteoblast.^{2a,b} The observed levels of clinical efficacy associated with bisphosphonate treatment have been attributed to, and appear to be limited by, osteoblast-mediated refilling of the existing resorption spaces left by the osteoclast.^{1a} Since its initial discovery over a decade ago, the key role of cathepsin K in osteoclast-mediated bone resorption has been firmly established.⁴ Compared to bisphosphonates, cathepsin K inhibition blocks bone resorption to a similar degree but reduces bone formation to a lesser extent.²⁰ Thus, a Cat K inhibitor would be a welcome addition to a physician's armamentarium by virtue of this unique mode of action. However, it still remains to be determined during ongoing clinical trials²¹ if a small molecule Cat K inhibitor will achieve greater fracture reduction efficacy than currently available therapies.

In summary, our efforts in this area have led to the identification of **31** (MK-1256), a nitrile-based inhibitor of Cat K built on a trans-2-substituted cyclohexanecarboxamide scaffold. Compound **31** is a reversible, potent (humanized rabbit Cat K^{10a,b} $IC_{50} = 0.62$ nM), and selective (>1100-fold vs human cathepsins B, L, S, C, H, V, and Z, 110-fold vs human cathepsin F) inhibitor of cathepsin K. This compound demonstrated an excellent pharmacokinetic profile across several animal species and achieved efficacy comparable to other known Cat K inhibitors in an OVX rhesus model of osteoporosis.

Experimental Section

General. *m*-Chloroperoxybenzoic acid (*m*-CPBA) was purified by washing a benzene solution of commercial material with two portions of pH 7.4 phosphate buffer followed by recrystallization from ether/hexanes. All other reagents were obtained commercially and were used without further purification. Proton (¹H NMR) magnetic resonance spectra were recorded on Bruker 400 and 500 MHz instruments. All spectra were recorded in acetone-*d*₆ (unless otherwise indicated) using residual solvent as the internal standard. Signal multiplicity was designated according to the following abbreviations: s = singlet, d = doublet, dd = doublet of doublets, ddd = doublet of doublet of doublets, t = triplet, q = quartet, dt = doublet of triplets, td = triplet of doublets, dq = doublet of quartets, m = multiplet, br = broad. Elemental analyses were provided by Prevalere Life Sciences Inc., Whitesboro, NY. Rotations were measured on a Perkin-Elmer model 241 polarimeter. Reactions were carried out with continuous stirring under a positive

pressure of nitrogen except where noted. Flash chromatography was carried out with silica gel 60, 230–400 mesh.

Enzyme Expression and Purification. See ref 10b.

Enzyme Activity Assays. See ref 10b.

Pharmacokinetic and Bioavailability Experiments. Single compounds were dosed orally as suspensions in 1% methocel and intravenously via the jugular vein as solutions in PEG-200/H₂O (3:2). Dosing volumes used for oral administration were 10 mL/kg for rats, 1 mL/kg for monkeys, and 5 mL/kg for dogs. Intravenous dosing volumes of 1 mL/kg were used for all species. Animals receiving the oral suspensions were fasted overnight prior to a.m. dosing. Plasma samples were collected at regular intervals and analyzed by LC-MS following a protein precipitation with 1.5 volumes of acetonitrile and centrifugation. All animal procedures were conducted in accordance with Institutional Animal Care and Use Committee guidelines.

Hepatocyte Incubations. For hepatocyte incubations, 1×10^6 cells diluted in 0.5 mL of Krebs–Henseleit buffer were first prepared at 37 °C for 20 min under 95:5 O₂/CO₂ (BOC gases; Montreal, Canada) in a 48-well plate, and then an amount of 5 μ L of 10 mM solution of compound dissolved in acetonitrile was added to each well to a final concentration of 50 μ M. After 2 h of incubation at 37 °C under 95:5 O₂/CO₂ atmosphere, one volume of acetonitrile was added in each well. A quenched incubation spiked with the parent compound and a blank were also prepared as controls. Once transferred, samples were centrifuged for 10 min at 14 000 rpm using an Eppendorf 5415C centrifuge (Hamburg, Germany), and the supernatant was used for LC/UV/MS analysis.

Diethyl {2-[(4R)-4-Benzyl-2-oxo-1,3-oxazolidin-3-yl]-2-oxoethyl}-phosphonate (7). *n*-BuLi (2.5 M in hexanes, 622 mL, 1550 mmol, 1 equiv) was added over 10–15 min to a –78 °C solution of (4R)-4-benzyl-1,3-oxazolidin-2-one (275 g, 1550 mmol) in THF (3.7 L) at a rate such that the internal temperature was maintained below –65 °C. The resulting yellow solution was stirred at this temperature for an additional 10 min prior to the rapid introduction of bromoacetyl bromide (135 mL, 1550 mmol, 1 equiv) over a period of 15 min. The mixture was then allowed to slowly attain room temperature, followed by stirring at room temperature overnight. Water (370 mL) was added, and the majority of the THF was removed by rotary evaporation. The residue was partitioned between ethyl acetate and water, and the layers were separated. The aqueous phase was extracted with an additional portion of ethyl acetate, and the combined organics were washed with water and brine, dried over Na₂SO₄, and concentrated. The residue was purified by filtration through a pad of silica gel in a large sintered glass funnel eluting with 20% ethyl acetate in hexanes to afford (4R)-4-benzyl-3-(bromoacetyl)-1,3-oxazolidin-2-one as a waxy solid (316 g, 68% yield). This material (316 g, 1060 mmol) and triethylphosphite (204 mL, 1170 mmol, 1.1 equiv) were heated together in refluxing toluene (740 mL) for 20 h. Concentration by rotary evaporation followed by hi-vac treatment with heating afforded the desired keto-phosphonate as a thick, yellow syrup (377 g) that was used directly in the next step.

(4R)-4-Benzyl-3-[(2E)-4-(benzyloxy)but-2-enoyl]-1,3-oxazolidin-2-one (8). Hünig's base (204 mL, 1170 mmol, 1.1 equiv) was added at 0 °C to a mixture of keto-phosphonate **7** (377 g, 1060 mmol) and anhydrous LiCl (49.4 g, 1170 mmol, 1.1 equiv) in CH₃CN (1 L). The mixture was mechanically stirred at this temperature for 10 min prior to the slow introduction of benzyloxyacetaldehyde (150 mL, 1060 mmol, 1 equiv) followed by stirring at room temperature overnight (12 h). Water was then added followed by extraction with ether (2 \times). The combined extracts were then vigorously stirred at room temperature with an equal volume of 1 M HCl for 1 h. Stirring with HCl is required to isomerize the (*Z*)-isomer, which is also produced in the reaction, to the desired (*E*)-isomer. The organic phase was then washed with brine and saturated NaHCO₃ solutions and dried over Na₂SO₄/MgSO₄. Concentration in vacuo and passage of the residue through a silica plug eluting with 1:1 ethyl acetate/hexanes yielded a colorless solid (372 g) upon trituration with ether. ¹H NMR (500 MHz, acetone-*d*₆) δ 7.57 (1H, d, *J* = 16 Hz), 7.43–7.27 (10H, m), 7.21–7.15 (1H, m), 4.84 (1H,

J = 8.2 Hz), 4.64 (2H, s), 4.43 (1H, t, *J* = 8.5 Hz), 4.32 (2H, m), 4.29 (1H, dd, *J* = 2.9, 8.9 Hz), 3.24 (1H, dd, *J* = 3.1, 14 Hz), 3.03 (1H, dd, *J* = 8.4, 14 Hz).

(4R)-4-Benzyl-3-[(1R,2R)-2-[(benzyloxy)methyl]-4-oxocyclohexyl]-carbonyl]-1,3-oxazolidin-2-one (9a). A 1.8 M solution of Et₂AlCl in toluene (812 mL, 1460 mmol, 1.4 equiv) was added slowly to a –78 °C solution of dienophile **8** (367 g, 1044 mmol) in CH₂Cl₂ (1100 mL). The resulting yellow solution was stirred at this temperature for 10 min prior to the slow introduction of 2-[(trimethylsilyloxy)-1,3-butadiene (520 g, 3.5 equiv) as a solution in CH₂Cl₂ (500 mL). After 16 h at –78 °C, the temperature was raised to –40 °C and a 1:1 mixture of 6 M HCl and THF (500 mL) was carefully added dropwise followed by an additional portion of 1:1 THF/6 M HCl (500 mL) after gas evolution had ceased. The mixture was then stirred at room temperature until TLC analysis indicated that hydrolysis of the enol–ether was complete (about 30 min). Ethyl acetate and Celite were added (to precipitate and capture polymeric material) with stirring at room temperature for 10–15 min followed by suction filtration and washing of the pad with ethyl acetate. The filtrate was washed with brine and dried over Na₂SO₄/MgSO₄. Concentration in vacuo and chromatography on silica gel (3 kg in a sintered glass funnel), eluting with 20% ethyl acetate/hexanes, afforded material that was swished with 15% ether in hexanes to afford 220 g of solid that was further purified by recrystallization from ethyl acetate/hexanes (250/650 mL) to afford the desired product as a colorless powder (160 g). Purification of the mother liquor concentrate by flash chromatography eluting with an increasing proportion of ethyl acetate in hexanes afforded an additional 42.1 g of product (202.1 g total, 45% yield over three steps) as a single diastereoisomer. ¹H NMR (400 MHz, acetone-*d*₆) δ 7.38–7.32 (6H, m), 7.31–7.25 (4H, m), 4.59–4.53 (1H, m), 4.47 (2H, q, *J* = 8.5 Hz), 4.19 (1H, dd, *J* = 3.0, 9.0 Hz), 4.15–4.09 (1H, m), 4.03 (1H, t, *J* = 8.6 Hz), 3.53–3.47 (2H, m), 3.13 (1H, dd, *J* = 3.4, 14 Hz), 2.97 (1H, dd, *J* = 8.2, 14 Hz), 2.70–2.60 (1H, m), 2.54–2.46 (1H, m), 2.44 (2H, d, *J* = 9.3 Hz), 2.41–2.29 (2H, m), 1.92–1.82 (1H, m). For the minor diastereomer: ¹H NMR (400 MHz, acetone-*d*₆) δ 7.40–7.22 (10H, m), 4.76 (1H, m), 4.55 (2H, m), 4.35 (1H, t, *J* = 8.4 Hz), 4.24–4.15 (2H, m), 3.56 (1H, dd, *J* = 9.4, 5.0 Hz), 3.49 (1H, dd, *J* = 9.4, 4.5 Hz), 3.16 (1H, dd, *J* = 14, 3.3 Hz), 2.70–2.57 (2H, m), 2.51 (1H, m), 2.48–2.39 (2H, m), 2.36–2.23 (2H, m), 1.78 (1H, m).

(4R)-4-Benzyl-3-[(1R,2R)-2-[(benzyloxy)methyl]-4,4-difluorocyclohexyl]carbonyl]-1,3-oxazolidin-2-one (10). Deoxofluor (21 mL, 110 mmol) was added slowly over 5 min to a 0 °C solution of ketone **9a** (18.7 g, 44.4 mmol) in CH₂Cl₂ (100 mL). After 2 h at this temperature, the reaction was quenched by the careful addition of an equal volume of ice–water. After separation of the phases, the aqueous layer was extracted with CH₂Cl₂ and the combined organics were washed with water and saturated aqueous NaHCO₃ and dried (Na₂SO₄). The methylene chloride solution containing the crude product was concentrated to a volume of 100 mL and treated with *m*-chloroperoxybenzoic acid (6.0 g, 35 mmol) with stirring at room temperature for 3 h to effect conversion of the fluoroalkene byproduct to the corresponding epoxide. Additional CH₂Cl₂ (100 mL) was then added followed by Me₂S (3 mL) and Ca(OH)₂ (20 g) with stirring at room temperature for 15 min. The slurry was filtered through Celite, and the filtrate was concentrated in vacuo. Flash chromatography of the residue on silica gel eluting with 1/3 ethyl acetate/hexanes yielded the title compound as a thick, colorless syrup (8.52 g, 43%). ¹H NMR (δ (500 MHz, acetone-*d*₆) 7.36–7.32 (6H, m), 7.26 (4H, dd, *J* = 7.3, 24 Hz), 4.54–4.50 (1H, m), 4.48–4.42 (2H, m), 4.19–4.15 (1H, m), 3.99 (1H, t, *J* = 8.6 Hz), 3.80–3.74 (1H, m), 3.47 (2H, d, *J* = 5.5 Hz), 3.13–3.09 (1H, m), 2.94 (1H, dd, *J* = 8.2, 14 Hz), 2.56–2.48 (1H, m), 2.26–2.12 (3H, m), 1.95–1.71 (3H, m).

{(1R,2R)-2-[(Benzyloxy)methyl]-4,4-difluorocyclohexyl}methanol (11). A solution of *n*-BuLi (2.5 M in hexanes, 10 mL) was added slowly to a solution of benzylmercaptan (3.6 mL, 40 mmol) in THF (40 mL) at 0 °C. The resulting pale-yellow solution was stirred at 0 °C for 10 min prior to the introduction of acyloxazolidinone **10** (8.52 g, 19.2 mmol) as a solution in THF (30 mL). After 10 min, a

solution of LiAlH_4 (1.0 M in THF, 22 mL) was slowly added to the reaction mixture with continued stirring at 0 °C for 45 min. Ice-water was then slowly added to destroy excess hydride followed by 6 M HCl (20 mL) to pH 1. The mixture was extracted with two portions of ethyl acetate, and the combined organics were washed with saturated aqueous NaCl and dried over $\text{Na}_2\text{SO}_4/\text{MgSO}_4$. Concentration in vacuo and flash chromatography of the residue on silica gel, eluting with 45/55 ethyl acetate/hexanes, afforded the title compound as a thick, colorless syrup (5.01 g, 96%). ^1H NMR (500 MHz, acetone- d_6) δ 7.36 (4H, m), 7.34–7.28 (1H, m), 4.56–4.49 (2H, m), 3.67–3.53 (5H, m), 2.20–2.12 (1H, m), 2.09–2.02 (1H, m), 1.91–1.71 (4H, m), 1.58–1.50 (2H, m).

(1R,2R)-2-[(Benzyloxy)methyl]-4,4-difluorocyclohexanecarbaldehyde (16). Dess–Martin periodinane (9.84 g, 23.2 mmol) was added to a solution of alcohol **11** (5.01 g, 20.2 mmol) in CH_2Cl_2 (50 mL) at 0 °C. The mixture was stirred at 0 °C for 5 min, then at room temperature for 1 h. Ethyl acetate (100 mL), water (100 mL), and a saturated aqueous solution of NaHCO_3 containing $\text{Na}_2\text{S}_2\text{O}_3 \cdot 5\text{H}_2\text{O}$ (28.9 g, 120 mmol) were added with stirring at room temperature for 30 min. The layers were separated, and the aqueous phase was extracted with additional ethyl acetate. The combined organics were washed with saturated NaCl aqueous solution and dried over $\text{Na}_2\text{SO}_4/\text{MgSO}_4$. Concentration in vacuo and flash chromatography on silica gel, eluting with 16/84 ethyl acetate/hexanes, gave the title compound as a colorless liquid (4.64 g, 86%). ^1H NMR (500 MHz, acetone- d_6) δ 9.66 (1H, d, $J = 3.0$ Hz), 7.37–7.33 (4H, m), 7.31–7.29 (1H, m), 4.52 (2H, m), 3.55 (1H, dd, $J = 4.8, 9.3$ Hz), 3.51–3.45 (1H, m), 2.43–2.33 (2H, m), 2.20–2.12 (2H, m), 1.98–1.66 (4H, m).

Ethyl 3-[(1R,2R)-2-[(Benzyloxy)methyl]-4,4-difluorocyclohexyl]-3-hydroxy-2-[4-(methylthio)phenyl]propanoate (18). A 2.1 M solution of *n*-BuLi (11 mL, 23 mmol) in hexanes was added slowly to a 0 °C solution of diisopropylamine (4.0 mL, 28 mmol) in THF (10 mL). Stirring was continued at this temperature for an additional 10 min prior to cooling to –78 °C. A solution of ethyl [4-(methylthio)phenyl]acetate (4.64 g, 18.9 mmol) in THF (15 mL) was then introduced, and the mixture was stirred at –78 °C for 10 min, –40 °C for 10 min, and finally 0 °C for 5 min. The solution was recooled to –78 °C, and a solution of aldehyde **16** (4.64 g, 18.9 mmol) in THF (15 mL) was added down the flask wall over 5 min. Stirring was continued at –78 °C for 30 min and then at –40 °C for 1 h. A saturated aqueous solution of NH_4Cl was added, and the reaction mixture was partitioned between ethyl acetate and water. The organic phase was washed with saturated aqueous NaCl solution and dried over $\text{Na}_2\text{SO}_4/\text{MgSO}_4$. Concentration in vacuo and flash chromatography on silica gel, eluting with 3/7 ethyl acetate/hexanes, gave the title compound as a single diastereomer in the form of a faint-yellow, thick syrup (5.09 g, 56%). ^1H NMR (400 MHz, acetone- d_6) δ 7.43–7.33 (5H, m), 7.33–7.29 (2H, m), 7.15–7.11 (2H, m), 4.66 (1H, m), 4.57–4.49 (2H, m), 4.16–4.00 (2H, m), 3.74 (2H, m), 3.45 (1H, m), 2.46 (3H, s), 2.13–1.95 (4H, overlapped m), 1.84–1.75 (2H, m), 1.73–1.63 (2H, m), 1.45 (1H, m), 1.17 (3H, t, $J = 7.1$ Hz).

Ethyl 3-[2-[(Benzyloxy)methyl]-4,4-difluorocyclohexyl]-2-[4-(methylthio)phenyl]-3-oxopropanoate (20). Oxalyl chloride (2.9 mL, 34 mmol) was added dropwise to a –78 °C solution of dimethyl sulfoxide (2.9 mL, 41 mmol) in CH_2Cl_2 (40 mL). Stirring was continued at –78 °C for an additional 10 min prior to the slow introduction down the flask wall of a solution of alcohol **18** (5.09 g, 10.6 mmol) and triethylamine (16 mL, 120 mmol) in CH_2Cl_2 (40 mL). The mixture was then held at –78 °C for 10 min followed by rapid warming to room temperature. The reaction vessel contents were then poured into 2 M HCl in a separatory funnel, the layers were shaken and separated, and the aqueous phase was extracted with an additional portion of CH_2Cl_2 . The combined organics were washed with water, dried (Na_2SO_4), and concentrated. Flash chromatography of the residue on silica gel, eluting with 1/4 ethyl acetate/hexanes, afforded the desired compound as a thick, tan colored syrup (4.43 g, 88%).

3-[(1R,2R)-2-[(Benzyloxy)methyl]-4,4-difluorocyclohexyl]-4-[4-(methylthio)phenyl]-1-(2,2,2-trifluoroethyl)-1H-pyrazol-5-ol (22). A slurry composed of keto-ester **20** (4.43 g, 9.31 mmol), 2,2,2-trifluoroethylhydrazine (70 wt % solution in water, 13 mL, 100 mmol, 10 equiv), 1,1,2,2-tetrachloroethane (100 mL), and MgSO_4 (50 g) was heated at 120 °C for 3 days. The mixture was then cooled in ice, and water (200 mL) was added followed by 6 M HCl to pH 1. The layers were separated, and the aqueous phase was extracted with two portions of CH_2Cl_2 . The combined organics were washed with water, dried (Na_2SO_4), and concentrated. Flash chromatography on silica gel, eluting with 15/85 acetone/benzene, yielded the title compound as a yellow foam (3.95 g, 81%). ^1H NMR (400 MHz, acetone- d_6) δ 9.66 (1H, br s), 7.36–7.26 (5H, m), 7.20 (4H, m), 4.78 (1H, m), 4.37 (1H, d, $J = 11$ Hz), 4.30 (1H, d, $J = 11$ Hz), 3.38 (2H, m), 2.75–2.92 (3H, m), 2.50 (3H, s), 2.41 (1H, m), 2.23 (1H, m), 2.00–1.75 (4H, m).

3-[(1R,2R)-2-[(Benzyloxy)methyl]-4,4-difluorocyclohexyl]-4-[4-(methylsulfonyl)phenyl]-1-(2,2,2-trifluoroethyl)-1H-pyrazol-5-yl Trifluoromethanesulfonate (24). A solution of hydroxypyrazole **22** (3.95 g, 7.50 mmol) and pyridine (0.95 mL, 12 mmol) in CH_2Cl_2 (30 mL) was cooled to 0 °C and treated with trifluoromethanesulfonic acid anhydride (1.5 mL, 9.2 mmol). After completion of the reaction, as indicated by TLC analysis (15 min at 0 °C), the reaction vessel contents were partitioned between water and CH_2Cl_2 , and the layers were separated. The aqueous layer was extracted with an additional portion of CH_2Cl_2 , and the combined organics were washed with water, dried (Na_2SO_4), and concentrated. Flash chromatography on silica gel, eluting with 15/85 ethyl acetate/hexanes, gave the corresponding triflate as a faint-yellow solid (4.36 g, 96%). This material was dissolved in CH_2Cl_2 (40 mL) and treated with *m*-chloroperoxybenzoic acid (2.62 g, 15.2 mmol) at 0 °C. The resulting slurry was stirred at 0 °C for 5 min and then at room temperature for 30 min before being diluted with CH_2Cl_2 (40 mL) and treated with dimethyl sulfide (0.25 mL) and $\text{Ca}(\text{OH})_2$ (9.0 g, 160 mmol). After being stirred at room temperature for 10 min, the mixture was filtered (Celite) and the filtrate was concentrated in vacuo. Flash chromatography on silica gel, eluting with 3/7 ethyl acetate/hexanes, gave the title compound as a colorless foam (4.54 g, 99%). ^1H NMR (400 MHz, acetone- d_6) δ 7.97 (2H, d, $J = 8.1$ Hz), 7.70 (2H, d, $J = 8.1$ Hz), 7.36–7.26 (3H, m), 7.19 (2H, m), 5.17–5.07 (2H, m), 4.35 (1H, d, $J = 12$ Hz), 4.28 (1H, d, $J = 12$ Hz), 3.37–3.27 (2H, m), 3.13 (3H, s), 2.97 (1H, m), 2.41 (1H, m), 2.22 (1H, m), 2.10–2.02 (2H, m), 2.00–1.92 (3H, m).

{(1R,2R)-5,5-Difluoro-2-[4-[4-(methylsulfonyl)phenyl]-1-(2,2,2-trifluoroethyl)-1H-pyrazol-3-yl]cyclohexyl}methanol (26). A mixture of triflate **24** (4.54 g, 6.58 mmol), triethylamine (1.3 mL, 9.3 mmol, 1.4 equiv), and 10% Pd/C (2.20 g) was stirred together in ethyl acetate (60 mL) under an atmosphere of hydrogen gas at room temperature for 16 h. Filtration through Celite, concentration of the filtrate, and flash chromatography on silica gel, eluting with 45/55 ethyl acetate/hexanes, yielded a colorless, thick syrup (2.15 g, 72%). This material (2.15 g, 3.97 mmol) and Pearlman's catalyst (1.0 g) were stirred together in ethyl acetate (50 mL) containing acetic acid (5 mL) under an atmosphere of hydrogen at room temperature for 20 h. The reaction mixture was then filtered through a Celite pad, and the filtrate was washed with saturated aqueous solutions of NaHCO_3 and NaCl before drying over Na_2SO_4 . Solvent removal in vacuo yielded the desired compound as a faint-yellow, thick syrup (1.64 g, 91%). ^1H NMR (400 MHz, acetone- d_6) δ 8.06 (1H, s), 7.96 (2H, d, $J = 8.4$ Hz), 7.79 (2H, d, $J = 8.4$ Hz), 5.08 (2H, q, $J = 8.8$ Hz), 3.70 (1H, m), 3.47 (1H, m), 3.36 (1H, m), 3.16 (3H, s), 3.09 (1H, m), 2.38 (1H, m), 2.25 (1H, m), 2.15–1.30 (5H, m).

(1R,2R)-5,5-Difluoro-N-(1-cyanocyclopropyl)-2-[4-[4-(methylsulfonyl)phenyl]-1-(2,2,2-trifluoroethyl)-1H-pyrazol-3-yl]cyclohexanecarboxamide (30). A solution of alcohol **26** (1.64 g, 3.63 mmol) in acetone (40 mL) was treated at 0 °C with Jones' reagent (3.8 mL) followed by stirring at room temperature for 30 min. Water was added, and the mixture was extracted with two portions of ethyl acetate. The combined organics were washed with water until no orange coloration was visible in the aqueous phase, followed

by washing with a saturated aqueous solution of NaCl before drying over Na₂SO₄/MgSO₄. Concentration in vacuo gave the desired carboxylic acid as a faint-yellow foam (1.69 g, 99%). This material was then combined with 1-aminocyclopropanecarbonitrile hydrochloride (1.16 g, 9.83 mmol) and HATU (1.72 g, 4.53 mmol) in DMF (10 mL), and the mixture was treated with diisopropylethylamine (3.2 mL, 18 mmol) with stirring at room temperature for 2.5 h. The reaction vessel contents were then partitioned between ethyl acetate and water, and the layers were separated. The aqueous phase was extracted with additional ethyl acetate, and the combined organics were washed with 2 M HCl, 10% Na₂CO₃, and saturated NaCl aqueous solutions, followed by drying over Na₂SO₄. Concentration in vacuo and flash chromatography on silica gel, eluting with 22.5/77.5 acetone/benzene, provided the title compound as a colorless powder (1.57 g, 82%) upon trituration with a mixture of hexanes and ether. [α]_D +2.2° (c 0.5, acetone). ¹H NMR (400 MHz, acetone-*d*₆) δ 8.03 (1H, s), 7.99 (2H, d, *J* = 8.5 Hz), 7.83 (1H, overlapped m), 7.81 (2H, d, *J* = 8.5 Hz), 5.05 (2H, q, *J* = 8.8 Hz), 3.36 (1H, m), 3.18 (3H, s), 3.12 (1H, m), 2.23 (1H, m), 2.15–1.95 (4H, m), 1.79 (1H, m), 1.37 (2H, m), 1.05 (1H, m), 0.81 (1H, m). MS (+ESI) 531.0 [M + H]⁺. Anal. (C₂₃H₂₃F₃N₄O₃S) C: calcd, 52.07; found, 51.97. H: calcd, 4.37; found, 4.34. N: calcd, 10.56; found, 10.10.

(4R)-4-Benzyl-3-((7R,8R)-7-[(benzyloxy)methyl]-1,4-dioxaspiro[4.5]dec-8-yl)carbonyl)-1,3-oxazolidin-2-one (12). TMSOTf (8.7 mL, 48 mmol, 10 mol %) was added to a 0 °C solution of ketone **9a** (202.1 g, 479.0 mmol) and 1,2-bis[trimethylsilyl(oxy)]ethane (147 mL, 600 mmol, 1.25 equiv) in CH₂Cl₂ (1 L). The mixture was stirred at room temperature for 12 h prior to the addition of Et₃N (11 mL, 80 mmol, 0.17 equiv) to quench the reaction. The mixture was then washed with saturated aqueous NaHCO₃ and dried over Na₂SO₄. Concentration by rotary evaporation followed by hi-vac application at 55 °C afforded the desired acetal as a thick, tan colored syrup (235.2 g, >99%). ¹H NMR (500 MHz, acetone-*d*₆) δ 7.36–7.22 (10H, m), 4.48 (1H, m), 4.42 (2H, s), 4.11 (1H, dd, *J* = 3.1, 8.9 Hz), 3.97 (4H, m), 3.94–3.90 (1H, t, *J* = 9.0 Hz), 3.67 (1H, m), 3.44–3.38 (2H, m), 3.09 (1H, dd, *J* = 3.3, 14 Hz), 2.92 (1H, dd, *J* = 8.3, 14 Hz), 2.52 (1H, m), 1.97 (1H, m), 1.86–1.76 (3H, m), 1.57–1.50 (1H, m), 1.44 (1H, t, *J* = 13 Hz).

{(7R,8R)-7-[(Benzyloxy)methyl]-1,4-dioxaspiro[4.5]dec-8-yl}methanol (13). *n*-BuLi (2.5 M in hexanes, 248 mL, 620 mmol, 1.3 equiv) was added dropwise to a 0 °C solution of ethanethiol (53 mL, 720 mmol, 1.5 equiv) in THF (900 mL). The resulting pale-yellow solution was stirred at 0 °C for 15 min prior to the slow introduction of the acyloxazolidinone **12** (222 g, 477 mmol) as a solution in THF (700 mL). The mixture was stirred at 0 °C until judged complete by TLC (20 min). A 1.0 M THF solution of LiAlH₄ (525 mL, 1.1 equiv) was then added dropwise with continued stirring at 0 °C. TLC analysis indicated that reduction of the thioester intermediate was complete within 1 h. Water (50 mL) was carefully added in a dropwise manner until gas evolution ceased and a gelatinous mass formed. Then 6 M HCl (380 mL, 1 mol of HCl per mol of hydride in LiAlH₄) was then carefully added dropwise to pH 3–4. Additional water was added, and the layers were separated. The aqueous phase was extracted with ethyl acetate, and the combined organics were washed with brine, dried over Na₂SO₄/MgSO₄, and concentrated. The residue was triturated with ether, and the resulting solid (recovered Evan's auxiliary) was collected by filtration (55.6 g, 66% recovery). The filtrate was concentrated, and the residue was chromatographed on silica gel (3 kg in a sintered glass funnel), eluting with 25/75 acetone/hexanes to afford the desired alcohol as a faint yellow syrup (119 g, 86% yield). ¹H NMR (500 MHz, acetone-*d*₆) δ 7.36 (4H, m), 7.29 (1H, m), 4.50 (2H, q, *J* = 9.6 Hz), 3.90 (4H, s), 3.61 (1H, m), 3.52–3.42 (3H, m), 3.43 (1H, t, *J* = 5.5 Hz), 1.88–1.72 (4H, m), 1.55–1.41 (4H, m).

(3R,4R)-3-[(Benzyloxy)methyl]-4-(hydroxymethyl)cyclohexanone (14). The acetal **13** (42.96 g, 147.1 mmol) was heated at 85 °C in a mixture of acetic acid (280 mL) and water (100 mL). TLC analysis revealed the reaction was complete after 2 h. The majority of the acetic acid was removed by rotary evaporation under hi-

vac, and the residue was dissolved in methanol (300 mL) and treated with K₂CO₃ (78 g) with stirring at room temperature. Water was added until the salts dissolved, and the methanol was removed by rotary evaporation under reduced pressure. The residue was partitioned between water and ethyl acetate. After separation of the layers, the aqueous phase was extracted with additional ethyl acetate and the combined organics were washed with brine, dried (Na₂SO₄/MgSO₄), and concentrated to afford a tan syrup (34.36 g, 95% yield). ¹H NMR (500 MHz, acetone-*d*₆) δ 7.36 (4H, m), 7.30 (1H, m), 4.56–4.50 (2H, m), 3.70 (1H, m), 3.66–3.60 (2H, m), 3.56 (1H, dd, *J* = 5.4, 9.3 Hz), 3.54–3.48 (1H, dd, *J* = 4.0, 9.3 Hz), 2.44–2.26 (4H, m), 2.13–2.07 (2H, m), 1.91 (1H, m), 1.67 (1H, m).

{(1R,2R)-2-[(Benzyloxy)methyl]-4,4-dichlorocyclohexyl}methanol (15). Hydrazine hydrate (150 mL, 20 equiv) was added to a slurry of powdered 4 Å molecular sieves (activated grade, Sigma-Aldrich) in anhydrous methanol (500 mL) with stirring at room temperature for 15 min. A solution of ketone **14** (34.46 g, 140 mmol) in methanol (300 mL) was then added with stirring at room temperature until the reaction was judged complete by TLC analysis (2 h). The mixture was filtered (Celite), and the pad was washed with methanol. The filtrate was then concentrated by rotary evaporation under hi-vac with heating at 50 °C. Meanwhile, Et₃N (69 mL, 500 mmol) was slowly added to a room temperature solution of anhydrous CuCl₂ (132.8 g, 990 mmol) in methanol (500 mL) with stirring for 30 min prior to cooling to 0 °C and additional stirring at this temperature for 2 h. The crude hydrazone from above was taken up in methanol (400 mL) and slowly added to this mixture over 25 min. Stirring was continued for an additional 45 min after warming the reaction flask contents to room temperature. Saturated NH₄Cl and 2 M HCl were added to dissolve the copper salts, followed by the addition of water and extraction with ethyl acetate (3×). The combined organics were washed with saturated NH₄Cl solution (3×) and brine, followed by drying over Na₂SO₄/MgSO₄. Concentration in vacuo and flash chromatography of the residue on silica gel (18 cm × 22 cm), eluting with 45/55 EtOAc/hexanes, gave the desired compound as a yellow oil (32.16 g, 76% yield). ¹H NMR (500 MHz, acetone-*d*₆) δ 7.37 (4H, m), 7.31 (1H, m), 4.51 (2H, q, *J* = 12 Hz), 3.65–3.51 (5H, m), 2.66 (1H, dt, *J* = 3.9, 14 Hz), 2.54 (1H, dq, *J* = 3.6, 14 Hz), 2.29–2.19 (2H, m), 1.86 (1H, m), 1.75 (1H, m), 1.56 (1H, m).

(1R,2R)-2-[(Benzyloxy)methyl]-4,4-dichlorocyclohexanecarbaldehyde (17). Dess–Martin periodinane (52.63 g, 124.1 mmol, 1.2 equiv) was added to a 0 °C solution of the alcohol **15** (32.16 g, 106.5 mmol) in CH₂Cl₂ (250 mL) followed by stirring at room temperature. TLC analysis indicated the reaction was complete after 1.5 h. Ethyl acetate (500 mL) and a solution composed of saturated NaHCO₃ (500 mL), water (200 mL), and Na₂O₃·5H₂O (170 g) were then added with vigorous stirring at room temperature for 30 min. The layers were then separated, the aqueous phase was extracted with additional ethyl acetate, and the combined organics were washed with brine and dried (Na₂SO₄/MgSO₄). Concentration in vacuo and flash chromatography under nitrogen pressure on silica gel (18 cm × 22 cm), eluting with 15/85 ethyl acetate/hexanes, gave the desired aldehyde as a colorless syrup (24.87 g, 78% yield). ¹H NMR (500 MHz, acetone-*d*₆) δ 9.65 (1H, d, *J* = 3.07 Hz), 7.39–7.32 (4H, m), 7.30 (1H, m), 4.50 (2H, m), 3.55 (1H, dd, *J* = 9.4, 4.9 Hz), 3.48 (1H, dd, *J* = 9.5, 5.5 Hz), 2.66 (1H, dt, *J* = 14, 3.1 Hz), 2.61 (1H, dq, *J* = 14, 3.2 Hz), 2.52–2.38 (2H, m), 2.36 (1H, m), 2.22 (1H, dd, *J* = 14, 12 Hz), 1.93–1.79 (2H, m).

Ethyl 3-[(1R,2R)-2-[(Benzyloxy)methyl]-4,4-dichlorocyclohexyl]-3-hydroxy-2-[4-(methylthio)phenyl]propanoate (19). *n*-BuLi (2.5 M in hexanes, 36 mL, 90 mmol) was added dropwise to a 0 °C solution of diisopropylamine (15 mL, 110 mmol) in THF (44 mL) with stirring at this temperature for 15 min. This solution was then cooled to –78 °C, and a solution of ethyl 4-(methylthio)phenylacetate (20.05 g, 95.5 mmol) in THF (80 mL) was added dropwise. The mixture was then warmed to 0 °C for 10 min prior to recooling to –78 °C. The aldehyde **17** (24.87 g, 82.9 mmol) was then added dropwise as a solution in THF (80 mL). Stirring was continued at –78 °C for 2 h with slow warming to –40 °C over 2 h. The reaction

vessel contents were finally warmed to 0 °C with stirring at this temperature for 10 min prior to quenching of the reaction with saturated NH₄Cl solution. The mixture was partitioned between ethyl acetate and water, and the layers were separated. The aqueous phase was extracted with additional ethyl acetate, and the combined organics were washed with brine before drying over Na₂SO₄/MgSO₄. Concentration in vacuo and flash chromatography on silica gel (18 cm × 24 cm), eluting with an increasing proportion of ethyl acetate in hexanes (1/4, 35/65, then 2/3), afforded the desired product as a single diastereomer at the hydroxyl and ester bearing stereocenters (33.85 g, 80% yield). ¹H NMR (400 MHz, acetone-*d*₆) δ 7.45–7.29 (7H, m), 7.17–7.11 (2H, m), 4.64 (1H, m), 4.58–4.52 (2H, m), 4.21 (1H, d, *J* = 6.06 Hz), 4.13 (1H, m), 4.06 (1H, m), 3.78–3.71 (2H, m), 3.48 (1H, m), 2.57–2.48 (2H, m), 2.47 (3H, s), 2.26 (1H, m), 1.97–1.88 (2H, m), 1.77 (1H, m), 1.24 (1H, m), 1.23–1.15 (3H, t, *J* = 7.0 Hz).

Ethyl 3-[(1*R*,2*R*)-2-[(benzyloxy)methyl]-4,4-dichlorocyclohexyl]-3-[4-(methylthio)phenyl]-3-oxopropanoate (21). Oxalyl chloride (20 mL, 3.2 equiv) was added dropwise over 20 min to a –78 °C solution of DMSO (20 mL) in CH₂Cl₂ (250 mL). Stirring was continued at this temperature for an additional 40 min prior to the rapid introduction, via cannula over 5 min, of a –78 °C solution of **19** (36.76 g, 72.1 mmol) and Et₃N (100 mL, 10 equiv) in CH₂Cl₂ (250 mL). Stirring at –78 °C was continued for 45 min before allowing the reaction vessel contents to warm to 0 °C over 1 h, followed by the addition of a 2 M solution of HCl (200 mL) to quench the reaction. The mixture was transferred to a separatory funnel, and the layers were separated. The aqueous phase was extracted with CH₂Cl₂, and the combined organics were washed with water and dried over Na₂SO₄. Concentration in vacuo and flash chromatography on silica gel (11 cm × 23 cm), eluting with 1/9 and then 1/3 ethyl acetate/hexanes, gave the keto-ester product as a thick, yellow syrup (35.53 g, 97% yield).

3-[(1*R*,2*R*)-2-[(benzyloxy)methyl]-4,4-dichlorocyclohexyl]-4-[4-(methylthio)phenyl]-1-(2,2,2-trifluoroethyl)-1*H*-pyrazol-5-ol (23). A mixture of keto-ester **21** (35.53 g, 70 mmol) and trifluoroethylhydrazine (70 wt % in water, 110 g, 10 equiv) in toluene (700 mL) was heated at 125 °C in a three-neck flask fitted with a pressure equalizing addition funnel containing 3 Å molecular sieves (215 g, round pellets, activated grade from Acros) and a reflux condenser placed on top of the addition funnel. Heating at reflux, at a rate sufficient to force the vapor phase up the entire length of the foil wrapped funnel sidearm, was continued until no more water was evident in the reaction flask (35 min). The reaction vessel contents were then cooled to 60 °C, and anhydrous MgSO₄ powder (36 g) was added directly to the reaction flask. Heating at reflux (oil bath temp = 125 °C) was then continued for 3.5 days before cooling to room temperature and filtering to remove the MgSO₄. Concentration of the filtrate and flash chromatography on silica gel (18 cm × 23 cm), eluting with 15/85 acetone/benzene, yielded the title compound as a yellow foam (25.16 g, 64% yield). ¹H NMR (500 MHz, acetone-*d*₆) δ 9.80 (1H, br s), 7.37 (1H, s), 7.35–7.24 (5H, m), 7.19 (4H, m), 4.75 (2H, m), 4.37 (1H, d, *J* = 12 Hz), 4.28 (1H, d, *J* = 12 Hz), 3.41–3.32 (2H, m), 2.80 (1H, overlapped m), 2.70 (1H, m), 2.59–2.49 (2H, m), 2.50 (3H, s), 2.34 (1H, m), 2.29 (1H, m), 1.91 (1H, m).

3-[(1*R*,2*R*)-2-[(benzyloxy)methyl]-4,4-dichlorocyclohexyl]-4-[4-(methylsulfonyl)phenyl]-1-(2,2,2-trifluoroethyl)-1*H*-pyrazol-5-yl-trifluoromethanesulfonate (25). Trifluoromethanesulfonic anhydride (9.1 mL, 54 mmol, 1.2 equiv) was added dropwise to a solution of hydroxypyrazole **23** (25.16 g, 45 mmol) and pyridine (5.5 mL, 68 mmol, 1.5 equiv) in CH₂Cl₂ (200 mL) at 0 °C, followed by stirring at room temperature for 30 min. The mixture was then partitioned between ether and water, and the layers were separated. The aqueous phase was extracted with additional ether, and the combined organics were dried over Na₂SO₄/MgSO₄. Concentration in vacuo and flash chromatography of the residue on silica gel, eluting with 1/4 ethyl acetate/hexanes, gave 3-[(1*R*,2*R*)-2-[(benzyloxy)methyl]-4,4-dichlorocyclohexyl]-4-[4-(methylthio)phenyl]-1-(2,2,2-trifluoroethyl)-1*H*-pyrazol-5-yl trifluoromethanesulfonate as a colorless foam (28.01 g, 90% yield). ¹H NMR (500 MHz, acetone-*d*₆) δ 7.37–7.22

(7H, m), 7.20–7.15 (2H, m), 5.12–5.03 (2H, m), 4.36 (1H, d, *J* = 12 Hz), 4.27 (1H, d, *J* = 12 Hz), 3.35 (1H, m), 3.28 (1H, m), 2.93 (1H, m), 2.82 (1H, m), 2.70 (1H, m), 2.43–2.28 (2H, m), 2.57 (1H, m), 2.52 (3H, s), 2.43–2.28 (2H, m). *m*-CPBA (14.3 g, 83.0 mmol, 2.1 equiv) was added portionwise to a solution of product from above (28.01 g, 40.5 mmol) in CH₂Cl₂ (200 mL) at 0 °C followed by stirring at room temperature until the reaction was judged to be complete by TLC analysis (1.5 h). Calcium hydroxide (54 g, 730 mmol) was added with stirring at room temperature for 20 min prior to filtration through Celite. Concentration in vacuo gave the title compound as a faint-yellow solid (26.95 g, 92% yield). ¹H NMR (400 MHz, acetone-*d*₆) δ 7.98 (2H, d, *J* = 8.2 Hz), 7.70 (2H, d, *J* = 8.2 Hz), 7.38–7.26 (3H, m), 7.24–7.17 (2H, m), 5.21–5.07 (2H, m), 4.36 (1H, d, *J* = 12 Hz), 4.28 (1H, d, *J* = 12 Hz), 3.37 (1H, dd, *J* = 9.4, 3.0 Hz), 3.31 (1H, dd, *J* = 9.4, 4.8 Hz), 3.14 (3H, s), 2.98 (1H, td, *J* = 12, 4.1 Hz), 2.82 (1H, narrow m), 2.70 (1H, dt, *J* = 14, 3.0 Hz), 2.63–2.52 (2H, m), 2.44 (1H, m), 2.36 (1H, m), 2.02 (1H, m).

{(1*R*,2*R*)-5,5-Dichloro-2-[4-[4-(methylsulfonyl)phenyl]-1-(2,2,2-trifluoroethyl)-1*H*-pyrazol-3-yl]cyclohexyl}methanol (27). To a mixture of triflate **25** (28.95 g, 39.13 mmol), 3 Å activated molecular sieve powder (54 g), and 10% Pd/C (27 g) under N₂ was added ethyl acetate (400 mL) with stirring at room temperature for 10 min. Et₃N (7.8 mL, 1.4 equiv) was then added, and the mixture was placed under an atmosphere of hydrogen (balloon) with stirring at room temperature overnight. The solids were removed by filtration through Celite, and the filtrate was concentrated. Flash chromatography of the residue on silica gel, eluting with 2/3 ethyl acetate/hexanes and then with pure ethyl acetate, afforded 3-[(1*R*,2*R*)-2-[(benzyloxy)methyl]-4,4-dichlorocyclohexyl]-4-[4-(methylsulfonyl)phenyl]-2-(2,2,2-trifluoroethyl)-1*H*-pyrazole as a colorless foam (14.15 g, 66% yield). ¹H NMR (400 MHz, acetone-*d*₆) δ 8.09 (1H, s), 7.89 (2H, d, *J* = 8.1 Hz), 7.74 (2H, d, *J* = 8.1 Hz), 7.34–7.23 (3H, m), 7.18–7.12 (2H, m), 5.10 (2H, q, *J* = 8.8 Hz), 4.34 (1H, d, *J* = 12 Hz), 4.22 (1H, d, *J* = 12 Hz), 3.37 (1H, dd, *J* = 9.4, 2.7 Hz), 3.31 (1H, dd, *J* = 9.3, 4.8 Hz), 3.19 (1H, td, *J* = 12, 3.8 Hz), 3.12 (3H, s), 2.74 (1H, m), 2.70–2.53 (2H, m), 2.52–2.38 (2H, m), 2.16 (1H, m), 2.02 (1H, m). Ethyl acetate (250 mL) and acetic acid (50 mL) were added to a flask containing Pearlman's catalyst (3.6 g) and the benzyl ether from above (14.15 g, 24.6 mmol) under an atmosphere of nitrogen. The atmosphere was then switched to hydrogen with stirring at room temperature overnight. Filtration (Celite) and concentration in vacuo provided the title alcohol as a colorless syrup (10.72 g, 90% yield). ¹H NMR (400 MHz, acetone-*d*₆) δ 8.06 (1H, s), 7.96 (2H, d, *J* = 8.3 Hz), 7.78 (2H, d, *J* = 8.3 Hz), 5.08 (2H, q, *J* = 8.8 Hz), 3.67 (1H, dd, *J* = 5.3, 4.3 Hz), 3.47 (1H, m), 3.34 (1H, m), 3.15 (3H, s), 3.09 (1H, td, *J* = 12, 3.9 Hz), 2.79 (1H, narrow m), 2.76 (1H, dt, *J* = 14, 3.0 Hz), 2.60–2.51 (2H, m), 2.38 (1H, m), 2.11 (1H, m), 1.92 (1H, m).

(1*R*,2*R*)-5,5-Dichloro-2-[4-[4-(methylsulfonyl)phenyl]-1-(2,2,2-trifluoroethyl)-1*H*-pyrazol-3-yl]cyclohexanecarboxylic acid (29). Jones' reagent (2.7 M, 29 mL, 2.7 equiv) was added dropwise at 0 °C to a solution of alcohol **27** (13.75 g, 28.30 mmol) in acetone (250 mL) followed by stirring at room temperature until the reaction was judged complete by TLC (1 h). The mixture was then partitioned between ethyl acetate and water, and the layers were separated. The aqueous phase was extracted with additional ethyl acetate, and the combined organics were washed with water until no color was visible in the organic phase (two to three washings). This was followed by washing with brine and drying of the organics over Na₂SO₄/MgSO₄. Concentration in vacuo gave the desired acid as a faint-yellow foam (13.45 g, 95% yield). ¹H NMR (400 MHz, acetone-*d*₆) δ 11.50 (1H, br), 8.03 (1H, s), 7.98 (2H, d, *J* = 8.3 Hz), 7.81 (2H, d, *J* = 8.3 Hz), 5.04 (2H, q, *J* = 8.8 Hz), 3.50 (1H, m), 3.42 (1H, m), 3.16 (3H, s), 2.91 (1H, dt, *J* = 14, 3.0 Hz), 2.60–2.44 (3H, m), 2.12–1.92 (2H, overlapped m).

(1*R*,2*R*)-5,5-Dichloro-*N*-(1-cyanocyclopropyl)-2-[4-[4-(methylsulfonyl)phenyl]-1-(2,2,2-trifluoroethyl)-1*H*-pyrazol-3-yl]cyclohexanecarboxamide (31). A mixture of carboxylic acid **29** (13.45 g, 26.95 mmol), HATU (11.27 g, 29.65 mmol, 1.1 equiv), and cyclopro-

pylaminonitrile (7.03 g, 59.3 mmol, 2.2 equiv) in DMF (150 mL) was treated with Hüning's base (18.8 mL, 4 equiv) with stirring at room temperature for 2 days. The mixture was then added to 10% HCl and extracted with ether (2×). The combined ether extracts were washed with saturated brine and sodium bicarbonate solutions, dried over Na₂SO₄, and concentrated. Flash chromatography on silica gel, eluting with 1/1 ethyl acetate/hexanes, afforded the final compound as a colorless powder (14.01 g, 96% yield). [α]_D +5.6° (c 0.5, acetone). ¹H NMR (500 MHz, acetone-*d*₆) δ 8.03 (1H, s), 8.01 (1H, overlapped br s), 7.98 (2H, d, *J* = 8.4 Hz), 7.80 (2H, d, *J* = 8.4 Hz), 5.06 (2H, q, *J* = 8.8 Hz), 3.43 (1H, m), 3.29 (1H, dt, *J* = 3.3, 12 Hz), 3.19 (3H, s), 2.71 (1H, m), 2.58–2.68 (3H, m), 2.00–1.94 (2H, m), 1.43–1.31 (2H, m), 1.10 (1H, m), 0.86 (1H, m). MS (+ESI) 563.1 [M + H]⁺. Anal. (C₂₃H₂₃Cl₂F₃N₄O₃S). C: calcd, 49.03; found, 48.92. H: calcd, 4.11; found, 4.01. N: calcd, 9.94; found 9.68.

References

- (1) (a) Gasser, J. The Relative Merits of Anabolics versus Anti-Resorptive Compounds: Where Our Targets Should Be, and Whether We Are Addressing Them. *Curr. Opin. Pharmacol.* **2006**, *6*, 313–318. (b) Bonnick, S. L. Osteoporosis in Men and Women. *Clin. Cornerstone* **2006**, *8*, 28–39.
- (2) (a) Henriksen, K.; Tanko, L. B.; Qvist, P.; Delmas, P. D.; Christiansen, C.; Karsdal, M. A. Assessment of Osteoclast Number and Function: Application in the Development of New and Improved Treatment Modalities for Bone Diseases. *Osteoporosis Int.* **2007**, *18*, 681–685. (b) Seeman, E.; Delmas, P. D. Bone Quality. The Material and Structural Basis of Bone Strength and Fragility. *N. Engl. J. Med.* **2006**, *354*, 2250–2261.
- (3) (a) Mathoo, M. R.; Becker, L.; Kumbhare, D.; Adachi, J. D. Therapeutic Advances in the Treatment of Osteoporosis. *Expert Opin. Ther. Pat.* **2007**, *17*, 277–285. (b) Grey, A. Emerging Pharmacologic Therapies for Osteoporosis. *Expert Opin. Emerging Drugs* **2007**, *12*, 493–508.
- (4) Troen, B. R. The Role of Cathepsin K in Normal Bone Resorption. *Drug News Perspect.* **2004**, *17*, 19–28.
- (5) (a) Gauthier, J.-Y.; Chauret, N.; Cromlish, W.; Desmarais, S.; Duong, L.; Falguyret, J.-P.; Kimmel, D.; Lamontagne, S.; Léger, S.; LeRiche, T.; Li, C.-S.; Massé, F.; McKay, D. J.; Nicoll-Griffith, D.; Oballa, R. M.; Palmer, J. T.; Percival, M. D.; Robichaud, J.; Riendeau, D.; Rodan, G. A.; Rodan, S. B.; Seto, C.; Thérien, M.; Truong, V.-L.; Venuti, M.; Wesolowski, G.; Young, R. N.; Zamboni, R.; Black, W. C. The Discovery of Odanacatib (MK-0822), a Selective Inhibitor of Cathepsin K. *Bioorg. Med. Chem. Lett.* **2008**, *18*, 923–928. (b) Li, C. S.; Deschenes, D.; Desmarais, S.; Falguyret, J.-P.; Gauthier, J. Y.; Kimmel, D. B.; Léger, S.; Massé, F.; McGrath, M. E.; McKay, D. J.; Percival, M. D.; Riendeau, D.; Rodan, S. B.; Thérien, M.; Truong, V.-L.; Wesolowski, G.; Zamboni, R.; Black, W. C. Identification of a Potent and Selective Non-Basic Cathepsin K Inhibitor. *Bioorg. Med. Chem. Lett.* **2006**, *16*, 1985–1989. (c) Palmer, J. T.; Bryant, C.; Wang, D.-X.; Davis, D. E.; Setti, E. L.; Rydzewski, R. M.; Venkatraman, S.; Tian, Z.-Q.; Burrill, L. C.; Mendonca, R. V.; Springman, E.; McCarter, J.; Chung, T.; Cheung, H.; McGrath, M.; Somoza, J.; Enriquez, P.; Yu, Z. W.; Strickley, R. M.; Liu, L.; Venuti, M. C.; Percival, M. D.; Falguyret, J.-P.; Prasit, P.; Oballa, R.; Riendeau, D.; Young, R. N.; Wesolowski, G.; Rodan, S. B.; Johnson, C.; Kimmel, D. B.; Rodan, G. Design and Synthesis of Tri-Ring P₃ Benzamide-Containing Aminonitriles as Potent, Selective, Orally Effective Inhibitors of Cathepsin K. *J. Med. Chem.* **2005**, *48*, 7520–7534.
- (6) (a) Crane, S. N.; Black, W. C.; Palmer, J. T.; Davis, D. E.; Setti, E.; Robichaud, J.; Paquet, J.; Oballa, R. M.; Bayly, C. I.; McKay, D. J.; Somoza, J. R.; Chauret, N.; Seto, C.; Scheiget, J.; Wesolowski, G.; Masse, F.; Desmarais, S.; Ouellet, M. β -Substituted Cyclohexanecarboxamide: A Nonpeptidic Framework for the Design of Potent Inhibitors of Cathepsin K. *J. Med. Chem.* **2006**, *49*, 1066–1079. (b) Robichaud, J.; Bayly, C. I.; Black, W. C.; Desmarais, S.; Léger, S.; Massé, F.; McKay, D. J.; Oballa, R. M.; Pâquet, J.; Percival, M. D.; Truchon, J.-F.; Wesolowski, G.; Crane, S. N. β -Substituted Cyclohexanecarboxamide Cathepsin K Inhibitors: Modification of the 1,2-Disubstituted Aromatic Core. *Bioorg. Med. Chem. Lett.* **2007**, *17*, 3146–3151.
- (7) (a) Falguyret, J.-P.; Oballa, R.; Okamoto, O.; Wesolowski, G.; Aubin, Y.; Rydzewski, R. M.; Prasit, P.; Riendeau, D.; Rodan, S. B.; Percival, M. D. Novel, Nonpeptidic Cyanamides as Potent and Reversible Inhibitors of Human Cathepsins K and L. *J. Med. Chem.* **2001**, *44*, 94–104. (b) The projected monkey and human bone resorption assay values were calculated by multiplying the bone resorption shift (BRS) by the humanized rabbit Cat K IC₅₀ value. The human, humanized rabbit, and monkey Cat K IC₅₀ values would be expected to be very similar (see refs 10a and 19b).
- (8) Wright, J. D.; Boudinot, F. D.; Ujhelyi, M. R. Measurement and Analysis of Unbound Drug Concentrations. *Clin. Pharmacokinet.* **1996**, *30*, 445–462.
- (9) Schechter, I.; Berger, A. On the Size of the Active Site in Proteases. *Biochem. Biophys. Res. Commun.* **1967**, *27*, 157–162.
- (10) (a) Humanized rabbit cathepsin K (hrab Cat K) was obtained by mutation of two active site amino acid residues of the rabbit enzyme to the corresponding human residues (Tyr⁶¹ → Asp⁶¹ and Val¹⁵⁷ → Leu¹⁵⁷). See ref 10b for expression and purification procedures. Cyclohexanecarboxamide based inhibitors were equipotent against humanized-rabbit and human Cat K. (b) Robichaud, J.; Oballa, R.; Prasit, P.; Falguyret, J.-P.; Percival, M. D.; Wesolowski, G.; Rodan, S. B.; Kimmel, D.; Johnson, C.; Bryant, C.; Venkatraman, S.; Setti, E.; Mendonca, R.; Palmer, J. T. A Novel Class of Nonpeptidic Biaryl Inhibitors of Human Cathepsin K. *J. Med. Chem.* **2003**, *46*, 3709–3737.
- (11) Case, D. A.; Pearlman, D. A.; Caldwell, J. W.; Cheatham, T. E., III.; Ross, W. S.; Simmerling, C. L.; Darden, T. A.; Merz, K. M.; Stanton, R. V.; Cheng, A. L.; Vincent, J. J.; Crowley, M.; Tsui, V.; Radmer, R. J.; Duan, Y.; Pitner, J.; Massova, I.; Seibel, G. L.; Singh, U. C.; Weiner, P. K.; Kollman, P. A. *AMBER*, version 6; University of California: San Francisco, CA, 1999.
- (12) Hale, K. J.; Jogiya, N.; Manaviar, S. Monamycin Synthetic Studies Part 1. An Enantiospecific Total Synthesis of (3*S*,5*S*)-5-Hydroxypiperazine Acid from D-Mannitol. *Tetrahedron Lett.* **1998**, *39*, 7163–7166.
- (13) (a) Armstrong, A.; Davies, N. G. M.; Martin, N. G.; Rutherford, A. P. Evaluation of Asymmetric Diels–Alder Approaches for the Synthesis of the Cyclohexene Subunit of CP-225,917 and CP-263,114. *Tetrahedron Lett.* **2003**, *44*, 3915–3918. (b) Evans, D. A.; Chapman, K. T.; Bisaha, J. Asymmetric Diels–Alder Cycloaddition Reactions with Chiral α,β -Unsaturated *N*-Acylloxazolidinones. *J. Am. Chem. Soc.* **1988**, *110*, 1238–1256.
- (14) Damon, R. E.; Coppola, G. M. Cleavage of *N*-Acyl Oxazolidinones. *Tetrahedron Lett.* **1990**, *31*, 2849–2852.
- (15) Takeda, T.; Sasaki, R.; Yamauchi, S.; Fujiwara, T. Transformation of Ketones and Aldehydes to *gem*-Dihalides via Hydrazones using Copper (II) Halides. *Tetrahedron* **1997**, *53*, 557–566.
- (16) Drayton, C. J. In *Comprehensive Heterocyclic Chemistry*, 1st ed; Pergamon: Oxford, U.K., 1984.
- (17) Radiolabeled **31** was prepared by using tritium instead of hydrogen gas in step d of Scheme 4.
- (18) (a) Lohr, J. W.; Willsky, G. R.; Acara, M. A. Renal Drug Metabolism. *Pharmacol. Rev.* **1998**, *50*, 107–141. (b) Nicoll-Griffith, D. A.; Gupta, N.; Twa, S. P.; Williams, H.; Trimble, L. A.; Yergey, J. A. Verlukast (MK-0679) Conjugation with Glutathione by Rat Liver and Kidney Cytosols and Excretion in the Bile. *Drug Metab. Dispos.* **1995**, *23*, 1085–1093.
- (19) (a) Binkley, N.; Kimmel, D.; Bruner, J.; Haffa, A.; Davidowitz, B.; Meng, C.; Schaffer, V.; Green, J. Zolendronate Prevents the Development of Absolute Osteopenia following Ovariectomy in Adult Rhesus Monkeys. *J. Bone Miner. Res.* **1998**, *13*, 1775–1782. (b) Guay, J.; Riendeau, D.; Mancini, J. A. Cloning and Expression of Rhesus Monkey Cathepsin K. *Bone* **1999**, *25*, 205–209.
- (20) Kumar, S.; Dare, L.; Vasko-Moser, J. A.; James, I. E.; Blake, S. M.; Rickard, D. J.; Hwang, S.-M.; Tomaszek, T.; Yamashita, D. S.; Marquis, R. W.; Oh, H.; Jeong, J. U.; Veber, D. F.; Gowen, M.; Lark, M. W.; Stroup, G. A Highly Potent Inhibitor of Cathepsin K (Relacatib) Reduces Biomarkers of Bone Resorption Both in Vitro and in an Acute Model of Elevated Bone Turnover in Vivo in Monkeys. *Bone* **2007**, *40*, 122–131.
- (21) Stoch, S. A.; Wagner, J. A. Cathepsin K Inhibitors: A Novel Target for Osteoporosis Therapy. *Clin. Pharmacol. Ther.* **2008**, *83*, 172–176.